# A Longitudinal Study on the Effects of Aducanumab on Alzheimer's Disease-Induced Brain Regional Atrophy and White Matter Hyperintensities

*Author*: Alessandro Nigi[1,2]
*Supervisors*: Leonor Cerda' Alberich[2], Maria Beser Robles[2]
*Examiner:* Jeroen C.W. Siero[1]
[1]*Department of Radiology, Center for Image Sciences, University Medical Center Utrecht (UMCU), Utrecht, the Netherlands.*
[2]*Biomadical Imaging Research Group, Medical Research Institute La Fe (IIS La Fe), Valencia, Spain.*
Email: a.nigi@students.uu.nl; Student number: 6358292

**ABSTRACT**

Alzheimer's Disease (AD) is the leading cause of dementia among elderly individuals. Despite extensive research, the exact underlying causes of the syndrome remain unknown, hindering the development of effective medications to prevent or alleviate its progression. In 2021, Biogen introduced aducanumab, a human monoclonal antibody that targets and clears neuritic plaques (NP) consisting of abnormal protein aggregates formed by amyloid β (Aβ). NP are well-established biomarkers specific to AD that consistently correlate with synaptic dysfunction, neuroinflammation, and neuronal loss in affected areas. However, clinical trials demonstrated that aducanumab does not lead to significant cognitive benefits. Despite the ineffectiveness of aducanumab on cognitive performance, no studies have investigated whether the treatment positively affects other frequently studied AD biomarkers, such as brain atrophy and the development of white matter hyperintensities (WMHs) associated with white matter (WM) damage. Examining the impact of the treatment on these structural AD features could provide insight into the role of NP and shed light on the extent of the effects resulting from their removal. In this study, we conducted a longitudinal investigation to explore the influence of aducanumab on AD-related atrophy in critical brain regions and the development of lobar WMHs. We compared the results from a group of aducanumab-treated AD (TAD) patients with those of normal AD (NAD) patients and individuals with mild cognitive impairment (MCI). Overall, our findings indicate that aducanumab does not mitigate regional atrophy. However, it effectively slows down the growth and spread of WMH volumes over a two-year treatment period. These results suggest that aducanumab may help limit WM damage, thereby mitigating the disrupted connectivity commonly observed in AD brains. This effect could potentially prevent the decline of cognitive abilities that heavily rely on intact WM, such as working memory. Our study concludes that combination therapy targeting multiple aspects of AD may be the most effective treatment.

## INTRODUCTION

Alzheimer's Disease (AD) is a prevalent neurodegenerative condition characterized by a gradual decline in memory and cognitive abilities, often accompanied by changes in behaviour and loss of functional skills[1,2]. The World Health Organization recognizes AD as a growing global health issue, affecting individuals, caregivers, and society at large. In the United States alone, there are expected to be approximately 13.8 million individuals diagnosed with AD by 2060[1–3].

The pathology of AD is characterized by two well-investigated features: neuritic plaques (NP) and neurofibrillary tangles (NFT)[4]. NP consist of abnormal extracellular deposits of amyloid β (Aβ) protein, while NFT consists of intracellular aggregated hyperphosphorylated tau protein. Several studies associated these features with neurodegeneration and reported them to emerge in the hippocampal formation, gradually spreading through anterior and posterior cortices[5–8]. According to the cascade hypothesis, this process leads to longitudinal degradation of the functional connectivity, structural connectivity and morphology of the affected regions[4]. For instance, many studies reported shrinkage or loss of brain tissue (atrophy) over time over the entire brain, especially in the areas affected earlier by AD, such as the hippocampus and the entorhinal cortex[6,8–12]. Other common consequences of NP spreading are white matter (WM) lesions, WM pathology and changes to white matter tracts[6,9,10,13–18]. As such, AD is often modelled as a "disconnection syndrome" or as "system degeneration". Despite advancements in understanding AD's pathogenesis, early detection, and disease progression, the precise factors driving the development and advancement of the disease remain incompletely understood.

High-resolution MRI has significantly advanced the recognition of AD in vivo features, enabling the analysis and accurate detection of AD even before the onset of clinical symptoms[9,19]. Particularly, in vivo biomarkers of specific (e.g. molecular biomarkers like NP) and non-specific (e.g. structural biomarker, like brain atrophy) AD-related pathologies can assist with the study of AD pathogenesis and progression in clinical trials[19].

Brain atrophy is one of the most studied non-specific biomarkers of AD[11,20]. Due to the NP cascade effect, the areas affected early in the disease progress, such as the hippocampus and the entorhinal cortex within the anterior parahippocampal gyrus and both related to memory formation and retrieval, exhibit the largest degree of disease-related damage. As such, hippocampal atrophy, consistently observed in AD patients, serves as a well-established and validated structural AD biomarker, displaying a reduction of 15-40% in volume in AD patients compared to healthy controls (HC) and an accelerated annual rate of atrophy (4.66% in AD compared to 1.41% in HC)[9]. Moreover, in AD patients, hippocampal volume correlates with clinical decline, the severity of cognitive disorder and episodic memory deficits. Other commonly affected areas are those related to decision-making, executive and cognitive functions, emotional regulation and language processing, such as the cingulate cortex, and the prefrontal cortex[9,12,21–27].

White matter hyperintensities (WMHs) are another popular target of research into AD pathogenesis and progression and appear as hyperintense WM areas on T2-weighted (T2W) fluid-attenuated inversion recovery (FLAIR) MRI[9,21,28]. WMHs are a non-specific biomarker of WM pathology (e.g. demyelination and axonal loss) and reflect cerebral small vessel diseases (CSVD), frequently used to study the manifestation of AD[29]. CSVD refers to

the wide spectrum of pathologies that affects small blood vessels in the brain[29,30]. WMHs highlight damage to white matter tracts and have been found to correlate with cognitive decline. Several studies have reported a strong association between WMHs volumes in the posterior, parietal and temporal lobes, AD stage and the extent of Aβ burden[1,14,29,31]. Therefore, WMHs are widely accepted as valid structural biomarkers of AD and, together with brain atrophy, may aid in supporting AD clinical diagnosis and assessing response to therapeutics[5,14,19,28–30,32].

Until recently, the approved drugs for AD treatment only aimed at attenuating symptoms rather than targeting the recognized pathological features of NFT and NP[1,33]. However, in 2021, the US Food and Drugs Administration (FDA) approved aducanumab (Aduhelm™, Biogen), the first disease-modifying therapy. Aducanumab is a human monoclonal antibody that selectively targets and clears brain NP. Researchers believed that given the fundamental role of NP in AD pathogenesis, reducing or completely removing brain NP would slow the cognitive decline associated with AD. However, while aducanumab successfully cleared NP in a dose-dependent manner, there was no clear evidence of subsequent cognitive improvements or slowing of cognitive decline in clinical trials[34–37]. Additionally, higher incidences of brain swelling intracerebral haemorrhages (amyloid-related imaging abnormalities, ARIA) were reported in patients undergoing the therapy, leading the European Medicines Agency (EMA) and Japan's Pharmaceuticals and Medical Devices Agency (PMDA) to decline the approval of aducanumab.

Despite aducanumab did not meet the main clinical endpoint of cognitive improvement, most research studying the effects of aducanumab focused solely on the molecular NP burden biomarker and cognitive scores, overlooking abnormalities of brain structure consistent with AD-related neurodegeneration, such as regional atrophy and WMHs. Exploring the effects of aducanumab on these structural biomarkers could clarify the actual extent of the treatment effects on the brain of AD patients. To date, no studies investigated whether aducanumab influenced these non-specific yet fundamental biomarkers of AD.

This work aims to investigate the effects of aducanumab on the time course of the core brain structure biomarkers of AD: brain regional atrophy and WMHs volumes. We conduct a longitudinal study comparing the time course of lobar WMHs volumes and of critical brain regional volumes of AD patients between a cohort of treated AD (TAD) patients receiving aducanumab, a cohort of normal AD (NAD) patients and a cohort of mildly cognitive impaired (MCI) patients[38,39]. Specifically, we analyze the volumes of the following regions of interest (ROIs): the hippocampus, the anterior and posterior parahippocampal gyrus, the angular gyrus, the precuneus, the anterior and posterior cingulate, the medial prefrontal cortex and the superior frontal gyrus, as they were consistently found to undergo significant atrophy in AD subjects[9,12,21–27]. Additionally, we compare the atrophy rates of the most commonly reported areas in AD studies: the hippocampus and the parahippocampal gyri[9].

Our results will shed light on whether aducanumab can mitigate AD-related structural damage by slowing down brain atrophy and the spread of WMHs. Furthermore, this analysis will further assess the role of amyloid-β-deposition in the progression of AD and elucidate its interaction with AD-related structural changes in the brain.

## METHODS

### *Study Design*

Briefly, this study analyses the brain regional and WMHs longitudinal volumes of the TAD group receiving aducanumab over two years of treatment and compares them to the NAD and MCI groups. After preprocessing the T1w and T2w-FLAIR MRI data via dicom to nifti conversion, denoising, registration of T2w-FLAIR to T1w and WMHs segmentation, we apply a voxel-based morphometry method to compute brain regional and lobar WMHs volumes for each subject at each time point. Then, we estimate the baseline regional and WMHs volumes and analyze the volumetric changes over time between the three groups to determine whether aducanumab influences the time course of brain morphology and structural connectivity (WM tracts) of the treated patients.

### *Subjects*

We obtained the data for the TAD group (n=13) from the EMBARK database in March 2023. EMBARK (NCT04241068) is a phase 3b, open-label, extension study ran by Biogen and is enrolling patients that previously participated in aducanumab studies (PRIME, EVOLVE, ENGAGE and EMERGE). EMBARK intends to assess the safety and efficacy of aducanumab after prolonged treatment interruption, such as changes in MRI morphometric measures of regional brain volume[40]. One subject lacked the last (9$^{th}$) acquisition and another subject the 4$^{th}$ and the 7$^{th}$.

For the NAD and MCI groups, we selected 13 AD and 13 MCI subjects aged 70 to 90 from the ADNI database (http://adni.loni.usc.edu) in May 2023. The selection criteria were that the NAD and MCI subjects underwent MR acquisitions at similar temporal distances to the TAD group and that covered a period of a minimum of one year. The ADNI database was established in 2003 by the National Institute of Aging, the National Institute of Biomedical Imaging and Bioengineering, the FDA, private pharmaceutical companies, and non-profit organizations[38,39]. The primary goal of ADNI was to test whether serial MRI, PET, and other biological markers, as well as clinical and neuropsychological assessments, can be combined to measure the progression of MCI and early AD. Determination of sensitive and specific markers of very early AD progression is intended to aid researchers and clinicians to develop new treatments, monitoring their effectiveness, as well as shorten the time and cost of clinical trials. ADNI is the result of the efforts of many co-investigators from a broad range of academic institutions and private corporations, and subjects have been recruited from over 50 sites across the United States and Canada[38,39]. For up-to-date information, see http://www.adni-info.org.

### *MRI Acquisition*

For the TAD group from the EMBARK trial, all MR images were obtained on a 3-T magnet (Philips Achieva, Philips Healthcare, The Netherlands) with a head coil. The T1W structural images were obtained using a 3D T1-weighted turbo field echo (TFE) sequence with TR = 6ms,

TE = 3ms, flip angle = 10°, anteroposterior sagittal encoding, field of view (FOV) = 240mm, acquisition matrix = 192 × 192, reconstruction matrix = 256 × 256, slices = 170, slice thickness = 1.2mm, voxel size = 1.25 × 1.25 × 1.2mm$^3$, approximate scan time = 6min. The T2W FLAIR images were obtained using a multi-slice T2-weighted inversion recovery (IR) turbo spin echo (TSE) sequence with TR = 11000ms, TE = 100ms, TI = 2800ms, flip angle = 90°, left-to-right axial encoding, FOV = 240mm, acquisition matrix = 256 × 256, reconstruction matrix = 256 × 256, slices = 27, slice thickness = 5mm, voxel size = = 5 × 0.94 × 1.5mm$^3$, approximate scan time = 2.5-4min. On average, each subject of the TAD group underwent a total of 9 MR acquisition sessions 8 to 12 weeks apart from each other, for a total of approximately 102 weeks (~25.5 months).

For the NAD and MCI group from the ADNI dataset, all MR images were obtained on a 3-T magnet (General Electric Signa HDxt and DISCOVERY MR750, General Electric Medical Systems, United States) with a head coil (GE 8HRBRAIN). The T1W structural images were obtained using a 3D T1-weighted accelerated sequence with TR = 7ms, TE = 3ms, flip angle = 11°, anteroposterior sagittal encoding, field of view (FOV) = 240mm, acquisition matrix = 256 × 256, reconstruction matrix = 256 × 256, slices = 196, slice thickness = 1.2mm, voxel size = 1.25 × 1.25 × 1.2mm$^3$. The T2W FLAIR images were obtained using a multi-slice T2-weigthed IR TSE sequence with TR = 11002ms, TE = 153.9ms, TI = 2250ms, flip angle = 90°, left-to-right axial encoding, FOV = 240mm, acquisition matrix = 256 × 256, reconstruction matrix = 256 × 256, slices = 42, slice thickness = 5mm, voxel size = = 5 × 0.94 × 1.5mm$^3$. On average, each subject of the NAD group underwent a total of 5 MR acquisition sessions 18-22 weeks apart from each other, for a total of approximately 100 weeks (~25 months).

*Data Preprocessing*

After converting the dicom files to nifti using dcm2niix[41], all the data underwent denoising via an anisotropic diffusion filter (ADF), which belongs to the group of "edge-preserving" filters[42,43]. ADF acts as a high-pass filter, removing high-frequency noise while leaving edges intact. Two parameters were tuned for the optimization of this filter: the number of iterations, which took a value from 1 to 3, and the diffusion rate or conductance, which took values of 0.5, 1, 1.5, and 2. Low values of the last parameter serve to preserve features of the image like high gradients or curvature[43].

Finally, each T2W-FLAIR image was registered to its corresponding T1W image using rigid registration with Elastix[44]. This step was necessary for segmenting the WMHs from the T2W-FLAIR images (*see Methods section "WMHs Segmentation")*[32].

*Regional Volumetry*

All T1W images underwent preprocessing using Statistical Parametric Mapping software (SPM) available at https://www.fil.ion.ucl.ac.uk/spm/software/spm12. SPM operates within MATLAB (MathWorks, Inc., Natick, MA, USA) and employs the voxel-based morphometry (VBM) technique[45]. VBM involves the spatial normalization of high-resolution T1W images from all participants to a common stereotactic space (MNI), extraction of normalized tissue types (GM, WM, and cerebrospinal fluid, CSF), smoothing of the extracted tissue maps, and subsequent statistical analyses to identify and draw conclusions about group differences[46].

Spatial normalization implies aligning all the image data to a standardized 3D stereotaxic space with a uniform 1 mm voxel size. This process ensures that corresponding brain structures can be examined across different individuals. Then, the images undergo automatic correction for field inhomogeneities using a correction factor of .001. Subsequently, the images are segmented into probabilistic maps representing different tissue types (GM, WM and cerebrospinal fluid CSF). To obtain binary masks of these tissue types, the probability maps are binarized using Otsu's method, which involves global image thresholding. The normalized and segmented images are then low-pass filtered using an isotropic Gaussian kernel with a 6 mm full-width at half-maximum (FWHM) Gaussian filter. This smoothing step serves to enhance the signal-to-noise ratio, as higher spatial frequencies may contain noise or irrelevant signals.

We employed a 143-region atlas based on the Harvard Oxford atlas, which is accessible through FSL (https://scalablebrainatlas.incf.org/human/HOA06). This atlas is aligned with the MNI space and provides information about the number of voxels occupied by GM, WM and CSF. During the normalization process, certain brain areas may undergo shrinkage or expansion to align the brain scans for comparison. To account for these secondary volume changes, the voxel values of each segmented mask and the atlas mask are adjusted by multiplying them with the Jacobian determinants obtained during spatial normalization[47]. These determinants contain parameters that capture the modifications made to specific brain regions to transform the raw data into the standardized stereotaxic space.

After registering the atlas to the subject's native space, we calculated the total subject's GM volume (GMV) and WM volume (WMV), and the number of GM voxels occupying each of the 143 atlas regions which, multiplied by the voxel size, provided the volume occupied by each region. From this volume, we calculated each region's volume relative to the total GMV of the brain, this ratio is used as the volume percentage of each region relative to the entire GMV.

*WMHs Segmentation and Volumetry*

To segment the WMHs, we used a U-Net with multi-scale highlighting foregrounds (HF)[32,48]. Briefly, this segmentation method aims to improve the detection of WMHs voxels with partial volume effects. The HF approach emphasizes the influence of the voxels lying on the lesion boundaries or within small lesions. The authors reported that their U-Net with HF method significantly improved the detection of WMHs voxels in small WMH clusters or at the edge of WMHs[32]. In terms of clinical utility, the method segmented WMH volumes that were significantly associated with cognitive performance and improved the classification between cognitive normal, mildly cognitive impaired and AD subjects. At the time of the publication, the U-Net with HF method achieved the best overall evaluation score among 39 methods submitted to the WMH segmentation challenge initially hosted by MICCAI 2017. The method is publicly available using Dockerhub (https://hub.docker.com/r/wmhchallenge/pgs) [30]. To apply the segmentation, we had to provide the T1w

and the T2w-FLAIR images registered to the respective T1w. These pairs of images enabled the algorithm to extract features such as spatial information, intensity information, and texture. The results were WMHs binary masks for each T2w-FLAIR image.

The estimation of WMHs volumes is an adaptation of the brain regional volumetry analysis previously reported (*see Methods section "Regional Volumetry").* Briefly, the data processing begins by spatially normalizing the registered T2W-FLAIR images to the common stereotactic MNI space. Then, we employed a 10-region lobar and cerebellar brain atlas (https://brainsuite.org/usclobesatlas) to which we included 6 additional areas corresponding to WM tracts within the cerebellum, namely the right and left inferior, middle and superior cerebellar peduncle, to increase the accuracy of WMHs localization (http://www.bmap.ucla.edu/portfolio/atlases/ICBM_DTI-81_Atlas/). After masking the T2W-FLAIR image with the WMHs binary mask obtained from the WMHs segmentation (*see Methods section "WMHs Segmentation"*) and registering the atlas to the subject's native space, we calculated the total subject's WMV and the number of WMHs voxels occupying each of the 16 atlas regions, which multiplied by the voxel size, provided the volume occupied by each WMHs region. Finally, we calculated each WMHs region's volume relative to the total WMHs volume (WMHsV) of the brain (WMHs/WMHsV) to describe the volume percentage of each WMHs region to the entire WMHs volume.

*Statistical Analysis*

The subjects in the NAD (MCI) group underwent 4 (5) scanning sessions (time points) 18-22 weeks apart from each other and spanning approximately one (two) years, while the TAD group included on average 9 timepoints 8-12 weeks apart per subject spanning approximately two years. To compare the effects of time and group on the regional and WMHs volumes of the groups, we removed the time points of the TAD group that did not have corresponding time points in the NAD (MCI) group. Hence, we obtained two pruned TAD datasets with 5 (6) time points per subject spaced 16-24 weeks apart and spanning approximately the same time period as the NAD (MCI) group of ~25 (~56) months. Consequently, we ran three distinct longitudinal analyses. The first analysis (Analysis 1) compares the results of the three groups from four time points over a one-year period (~56 weeks). The second analysis (Analysis 2) compares the results only for the TAD and MCI groups from five time points over a two-year period (~106 weeks). The last analysis (Analysis 3) reports the results only for the TAD group from nine time points over a two-year period (~106 weeks).

We used repeated measures ANOVA (rmANOVA) to assess significant time and/or group effects on the volumes of the ROIs and the WMHs in the three groups[49]. rmANOVA is a research design that involves multiple measures of the same variable taken on the same subjects over more than two time periods, such as a longitudinal study to assess change over time[49]. Before running the statistical analysis, we adapted the number of time points of the TAD dataset to those of the NAD and MCI datasets (*see Methods section "Dataset Preparation"*).

To assess time effects, we ran rmANOVA on each group. To assess group effects, we applied rmANOVA on the combined TAD NAD and TAD MCI groups. We then compared the group's results to assess if and which volumes show significantly different time courses between the three groups. We attributed significantly different time courses of the same region or lobar WMHs volumes between the groups to the effects of aducanumab or AD. All the statistical tests were implemented using Matlab 2020b. We applied the Greenhouse-Geisser method for epsilon correction to the p-values to account for the non-sphericity of the data[50].

We also estimated the average rate of atrophy by computing the ratio between the baseline hippocampal volume and the hippocampal volume after one year or, when applicable, by estimating the average over two years. We used paired student t-tests to assess differences in corresponding regional or lobar WMHs volumes at baseline and in annual atrophy rates between groups.

## RESULTS

### Regional Volumetry

*Baseline Regional Volumes*

The baseline volumes of the anterior parahippocampal gyrus and the posterior hippocampal gyrus were significantly smaller ($p < 0.5$) in the TAD group (MN = 4.64mm$^3$, SD = 0.66; MN = 2.60mm$^3$; SD = 0.34) than in the MCI group. The baseline volumes of the anterior cingulate, angular gyrus and medial frontal cortex were significantly larger ($p < .05$) in the TAD group (MN = 9.1mm$^3$, SD = 0.86, MN = 7.93mm$^3$, SD = 0.88; MN = 3.74mm$^3$, SD = 0.27) than in the NAD group (MN = 7.69mm$^3$, SD = 1.3; MN = 7.06mm$^3$, SD = 0.89; MN = 3.36mm$^3$, SD = 0.35).

*Analysis 1 (one year, four time points: TAD, NAD, MCI)*

Considering the TAD and NAD groups together, there were no statistically significant group differences in the regional volumes and region/brain percentage (Fig, 1A). In the TAD and MCI groups together, there was a statistically significant group effect on the atrophy of the hippocampus ($F(3,3) = 5.5$, $p < .05$); and in the region/brain percentage of the hippocampus ($F(3,3) = 6.04$, $p < .05$).

As shown in Fig. 2A, for the TAD group alone, there was statistically significant atrophy in the hippocampus, the anterior parahippocampal gyrus, the posterior parahippocampal gyrus, the posterior cingulate cortex, the anterior cingulate cortex, the precuneus and the angular gyrus ($F(3) = 29.17$, $p < .001$; $F(3) = 20.75$, $p < .001$; $F(3) = 5.29$, $p < .05$; $F(3) = 7.54$, $p < .001$; $F(3) = 4.3$, $p < .05$; $F(3) = 3.22$, $p < .05$, $F(3) = 7.2$, $p < .001$); and significant reductions in the region/brain percentage of the hippocampus, the precuneus and the angular gyrus ($F(3) = 4.04$, $p < .05$; $F(3) = 4.38$, $p < .05$; $F(3) = 3.59$, $p < .05$). For the NAD group alone, there was a statistically significant difference in the volumes of the hippocampus and the anterior parahippocampal gyrus ($F(3) = 13.05$, $p < .001$; $F(3) = 3.93$, $p < .05$); and in the region/brain percentage of the hippocampus ($F(3) = 8.33$, $p < .001$). For the CAD group alone, there was no statistically significant difference in the volume of the ROIs; and a significant difference in the region/brain percentage of the posterior cingulate cortex ($F(3) = 3.02$, $p < .05$).

| REGIONAL VOLUMETRY | | | | |
|---|---|---|---|---|
| | VOLUME | | PERCENTAGE | |
| | p < .05 | p < .001 | p < .05 | p < .001 |
| **(A)** | | | | |
| | **ANALYSIS 1** (one year, four timepoints: TAD, NAD, MCI) | | | |
| **TAD (time)** | Anterior cingulate cortex<br>Praecuneus<br>Posterior parahippocampal gyrus | Hippocampus<br>Anterior parahippocampal gyrus<br>Posterior cingulate cortex<br>Angular gyrus | Hippocampus<br>Precuneus<br>Angular gyrus | - |
| **NAD (time)** | Anterior parahippocampal gyrus | Hippocampus | - | Hippocampus |
| **MCI (time)** | - | - | Posterior cingulate cortex | - |
| **TAD vs NAD (group)** | - | - | - | - |
| **TAD vs MCI (group)** | Hippocampus | - | Hippocampus | |
| **(B)** | | | | |
| | **ANALYSIS 2** (two years, five timepoints: TAD, MCI) | | | |
| **TAD (time)** | Medial frontal cortex | Hippocampus<br>Anterior parahippocampal gyrus<br>Posterior parahippocampal gyrus<br>Posterior cingulate cortex<br>Anterior cingulate cortex<br>Precuneus<br>Angular gyrus | - | - |
| **MCI (time)** | - | - | Hippocampus<br>Posterior cingulate cortex<br>Precuneus | - |
| **TAD vs MCI (group)** | Posterior cingulate cortex<br>Precuneus<br>Angular gyrus<br>Medial frontal cortex<br>Posterior parahippocampal gyrus | Hippocampus<br>Anterior parahippocampal gyrus | - | - |
| **(C)** | | | | |
| | **ANALYSIS 3** (two years, nine timepoints: TAD) | | | |
| **TAD (time)** | Anterior cingulate cortex<br>Precuneus<br>Angular gyrus<br>Medial frontal cortex | Hippocampus<br>Anterior parahippocampal gyrus<br>Posterior cingulate cortex | - | - |

**Table 1.** Time and group effects on brain regions undergoing significant atrophy in the **A)** TAD, NAD and MCI groups over the first year of treatment, four timepoints; **B)** TAD and MCI groups over two years of treatment, five timepoints; **C)** TAD group over two years of treatment, nine timepoints. Patients receiving aducanumab in the TAD group experience a degree of regional atrophy comparable and superior to the NAD group and significantly higher than the MCI group, indicating no treatment effects.

| WMHs VOLUMETRY | | | | |
|---|---|---|---|---|
| | VOLUME | | PERCENTAGE | |
| | p < .05 | p < .001 | p < .05 | p < .001 |
| **(A)** | | | | |
| | **ANALYSIS 1** (one year, four timepoints: TAD, NAD, MCI) | | | |
| **TAD (time)** | - | - | - | - |
| **NAD (time)** | Right frontal lobe<br>Left frontal lobe<br>Right parietal lobe<br>Total WMHs | - | Right occipital lobe<br>Right temporal lobe | - |
| **MCI (time)** | Right temporal lobe | | Right frontal lobe | |
| **TAD vs NAD (group)** | - | - | - | - |
| **TAD vs MCI (group)** | - | - | - | - |
| **(B)** | | | | |
| | **ANALYSIS 2** (two years, five timepoints: TAD, MCI) | | | |
| **TAD (time)** | Left frontal lobe<br>Total WMHs | - | - | - |
| **MCI (time)** | Right frontal lobe<br>Right parietal lobe<br>Left parietal lobe<br>Right temporal lobe | Total WMHs | - | - |
| **TAD vs MCI (group)** | - | - | - | - |
| **(C)** | | | | |
| | **ANALYSIS 3** (two years, nine timepoints: TAD) | | | |
| **TAD (time)** | Left frontal lobe | - | - | - |

**Table 2.** Time and group effects on lobar and total WMHs volumes in the **A)** TAD, NAD and MCI groups over the first year of treatment, four timepoints; **B)** TAD and MCI groups over two years of treatment, five timepoints; **C)** TAD group over two years of treatment, nine timepoints. Patients receiving aducanumab in the TAD group exhibit WMHs volume growths comparable to the MCI group and smaller than the NAD group. These finding suggest that the treatment could be limiting the spread of WMHs, mitigating WM tract damage.

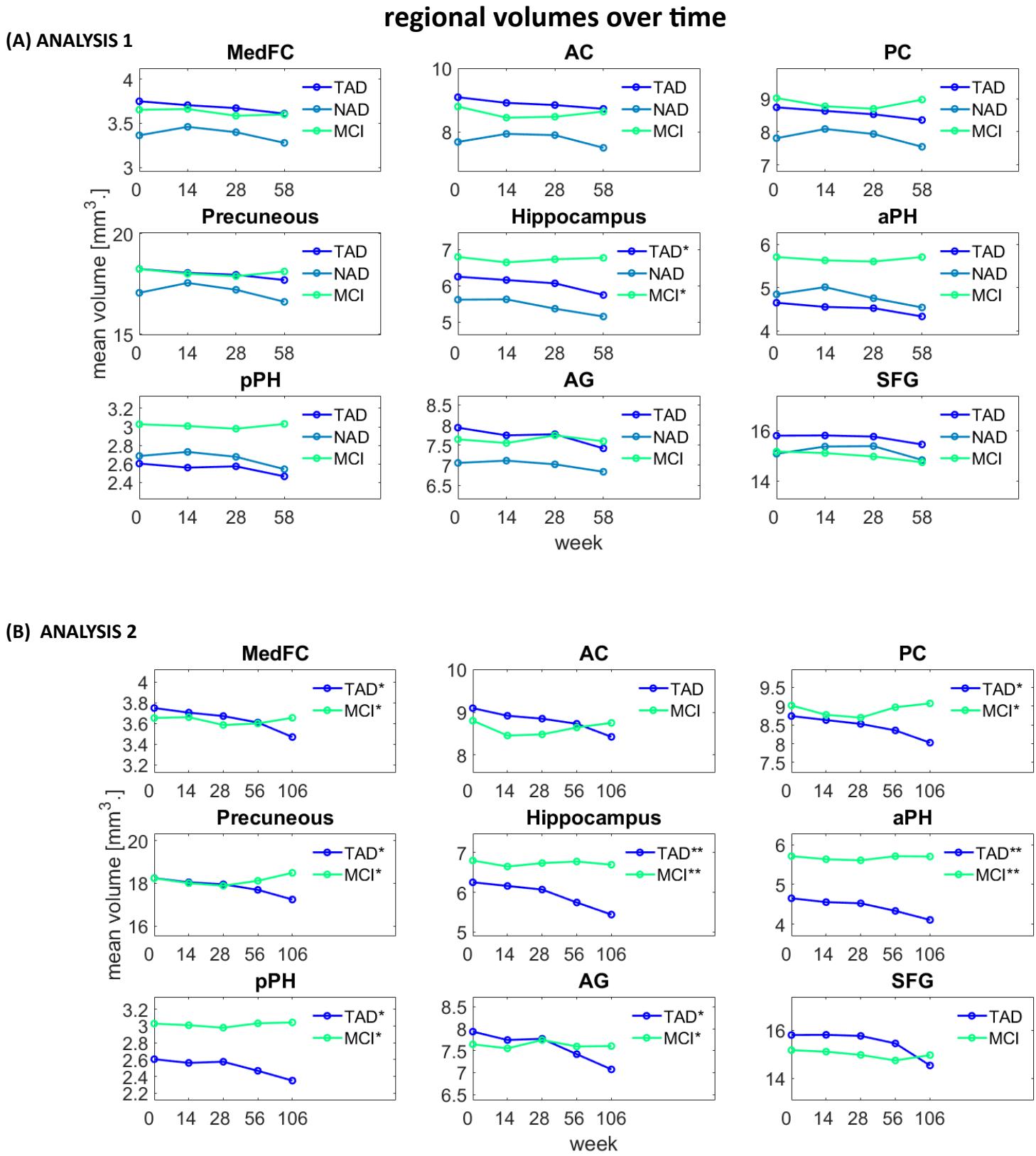


**Figure 1.** Regional volumes for of the medial frontal cortex (MedFC), anterior cingulate (AC), posterior cingulate (PC), precuneus, hippocampus, anterior parahippocampal gyrus (aPH), posterior parahippocampal gyrus (pPH), angular gyrus (AG) and superior frontal gyrus (SFG) in **A)** Analysis 1 (one year, four time points) and **B)** Analysis 2 (two years, five time points). * and ** Indicates significant ($p < .05$, $p < .001$) group differences. Overall, the atrophy patterns in the TAD group are comparable to the NAD patients, suggesting no treatment effects.

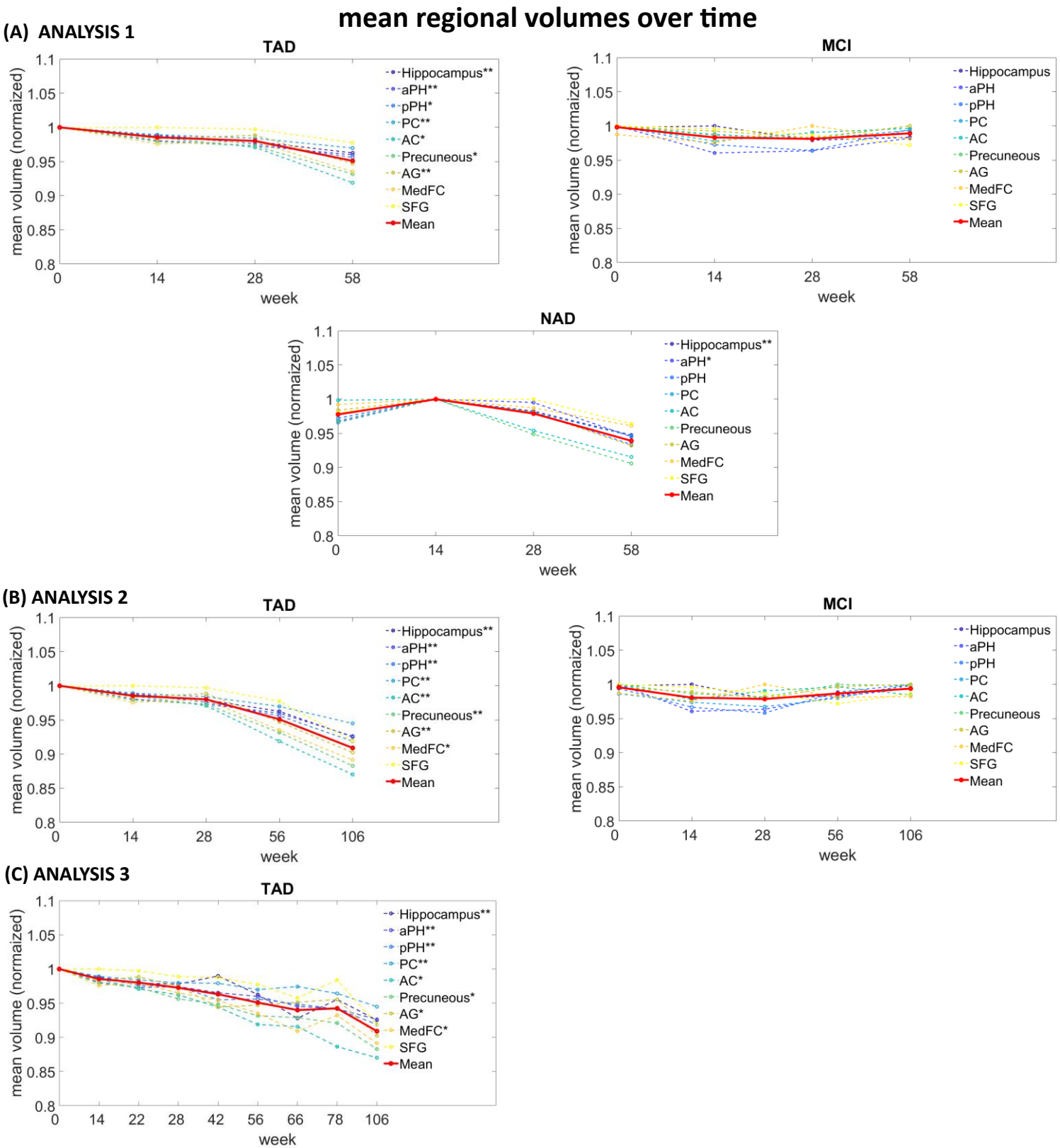


**Figure 2.** Mean regional volumes in **A)** Analysis 1 (one year, four time points), **B)** Analysis 2 (two years, five time points) and **C)** Analysis 3 (two years, nine time points). * and ** Indicate significant ($p < .05$, $p < .001$) time effects. Overall, the mean atrophy patterns in the TAD group are comparable to the NAD group, suggesting that aducanumab does not mitigate AD-related volume loss.

*Analysis 2 (two years, five time points: TAD, MCI)*

There were significant interaction effects between time and clinical group for the TAD and MCI groups in the atrophy of the hippocampus, the anterior parahippocampal gyrus, the posterior parahippocampal gyrus, the posterior cingulate cortex, the precuneus, the angular gyrus and the medial frontal cortex ($F(4,4) = 10.38$, $p < .001$; $F(4,4) = 6.38$, $p < .001$; $F(4,4) = 4.64$, $p < .05$; $F(4,4) = 4.88$, $p < .05$, $F(4,4) = 3.56$, $p < .05$; $F(4,4) = 3.61$, $p < .05$; $F(4,4) = 2.98$, $p < .05$); and there were no region/brain percentage differences in the ROIs (Fig. 1B and Table 1).

As shown in Fig. 2B, for the TAD group alone, there was statistically significant atrophy in the hippocampus, the anterior parahippocampal gyrus, the posterior parahippocampal gyrus, the posterior cingulate cortex, the anterior cingulate cortex, the precuneus, the angular gyrus and the medial frontal cortex ($F(4) = 40.60$, $p < .001$; $F(4) = 45.55$, $p < .001$; $F(4) = 9.00$, $p < .001$; $F(4) = 13.86$, $p < .001$; $F(4) = 10.49$, $p < .001$; $F(4) = 7.82$, $p < .001$; $F(4) = 14.37$, $p < .001$, $F(4) = 5.58$, $p < .05$); there were no significant region/brain percentage changes on the ROIs. For the MCI group alone, there was no significant atrophy in the ROIs. However, there were significant region/brain percentage reductions in the hippocampus, the posterior cingulate cortex and the precuneus ($F(4) = 3.27$, $p < .05$, $F(4) = 2.65$, $p < .05$; $F(4) = 3.12$, $p < .05$).

*Analysis 3 (two years, nine time points: TAD)*

There was statistically significant atrophy in the hippocampus, the anterior parahippocampal gyrus, the posterior cingulate cortex, the anterior cingulate cortex, the precuneus, the angular gyrus and the medial frontal cortex ($F(8) = 22.25$, $p < .001$; $F(8) = 19.89$, $p < .001$; $F(8) = 8.89$, $p < .001$; $F(8) = 4.99$, $p < .05$; $F(8) = 4.24$, $p < .05$; $F(8) = 6.30$, $p < .05$; $F(8) = 3.53$, $p < .05$). There were no significant region/brain percentage reductions in the ROIs (Fig. 2C).

**Annual Atrophy Rates**

*One Year: TAD, NAD, MCI*

There were no significant differences between the regional annual atrophy rates in terms of volume percentage loss in the TAD and NAD groups. Conversely, there was a significant difference in the hippocampal ($p < .001$) and anterior parahippocampal ($p < .05$) atrophy rates between the TAD (MN = 8.01, SD = 3.39; MN = 6.81, SD = 3.39) and the MCI (MN = 0.09, SD = 6.25; MN = 0.01, SD = 2.23) group.

*Two Years: TAD, MCI*

The mean rates of atrophy over two years of the hippocampus, the anterior parahippocampal gyrus and the posterior parahippocampal gyrus in terms of volume percentage loss in the TAD (MN = 6.65, SD = 5.84; MN = 5.87, SD = 2.01; MN = 4.23, SD = 3.09) and MCI (MN = 0.64, SD = 5.55; MN = 0.01%, SD = 3.43, MN = -0.34, SD = 3.31) group were significantly different ($p < .05$).

**WMHs Volumetry**

*Baseline WMHs Volumes*

The WMHs volumes in the right occipital lobe were significantly larger ($p < .05$) in the MCI (MN = 2.72mm$^3$, SD = 1.49) than in the TAD group (MN = 1.27mm$^3$, SD = 1.32). The WMHs volumes in the right frontal lobe, right parietal lobe, left parietal lobe right occipital lobe and left occipital lobe and the total WMHs volume were significantly larger ($p < .05$, $p < .001$, $p < .001$, $p < .001$, $p < .05$, $p < .05$) in the NAD (MN = 19.48mm$^3$, SD = 13.49; MN = 11.23mm$^3$, SD = 8.15; MN = 11.15mm$^3$, SD = 7.58; MN = 4.98mm$^3$, SD = 3.6; MN = 5/36, SD = 4.47; MN = 74mm$^3$, SD = 44.5) group compared to the TAD group (MN = 8.33mm$^3$, SD = 8.62; MN = 2.3mm$^3$, SD = 3.45; MN = 2.53mm$^3$, SD = 3.38; MN = 1.27mm$^3$, SD = 4.6; MN = 1.61mm$^3$, SD = 1.51; MN = 25.8mm$^3$, SD = 23.26).

*Analysis 1 (one year, four time points: TAD, NAD, MCI)*

There were no statistically significant group differences between the TAD and NAD groups taken together and between the TAD and MCI groups taken together (Fig. 3A and Table 2).

As shown in Fig. 4A, for the TAD group alone, there were no statistically significant changes in the WMHs volumes and percentages over time. For the NAD group alone, there was a statistically significant increase in the WMHs volumes of the right frontal lobe, left frontal lobe, right parietal lobe and total WMHs ($F(3) = 4.658$, $p < .05$; $F(3) = 5.55$, $p < .05$; $F(3) = 3.7$, $p < .05$; $F(3) = 4.5$, $p < .05$); and in the WMHs/WMHsV percentage of the right occipital lobe and right temporal lobe ($F(3) = 6.07$, $p < .05$; $F(3) = 3.58$, $p < .05$). For the MCI group alone, there was a statistically significant increase in the WMHs volumes of the right temporal lobe ($F(3) = 4.55$, $p < .05$); and in the WMHs/total WMHs percentage of the right frontal lobe ($F(3) = 3.23$, $p < .05$).

*Analysis 2 (two years, five time points: TAD, MCI)*

There were no significant interaction effects between time and clinical group on the WMHs volumes in the combined TAD and MCI groups (Fig. 3B).

As shown in Fig. 4B, for the TAD group alone, there was a statistically significant increase in the WMHs volumes of the left frontal lobe and total WMHs ($F(4) = 3.75$, $p < .05$; and $F(4) = 3.32$, $p < .05$); and in the WMHs/WMHsV percentage of the total WMHs ($F(4) = 3.27$, $p < .05$). For the MCI group alone, there was a statistically significant increase in the WMHs volumes of the right frontal lobe, right parietal lobe, left parietal lobe, right temporal lobe and total WMHs ($F(4) = 4.13$, $p < .05$; $F(4) = 5.5$, $p < .05$; $F(4) = 5.48$, $p < .05$; $F(4) = 2.95$, $p < .05$; $F(4) = 6.21$, $p < .001$). There were no significant WMHs/WMHsV percentage changes.

*Analysis 3 (two years, nine time points: TAD)*

There was a statistically significant increase in the WMHs volumes in the left frontal lobe ($F(8) = 2.8$, $p < .05$). There were no significant WMHs/WMHsV percentage changes (Fig. 4C).

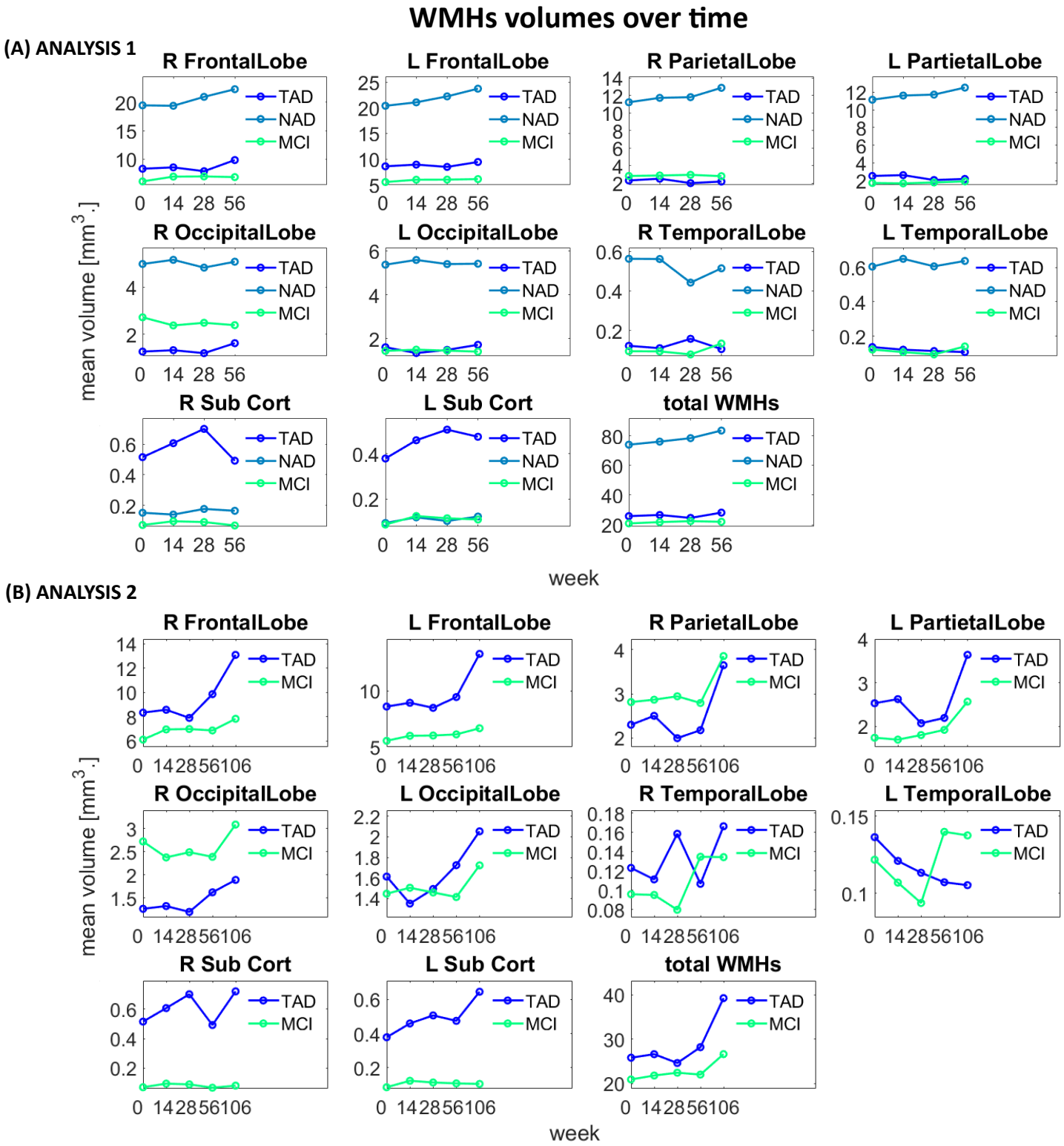


**Figure 3.** Lobar WMHs volumes in **A)** Analysis 1 (one year, four time points) and **B)** Analysis 2 (two years, five time points). RmANOVA did not report any significant group difference. Generally, WMHs volumes in the TAD group do not increase significantly over time, suggesting a treatment effect in limiting WM damage.

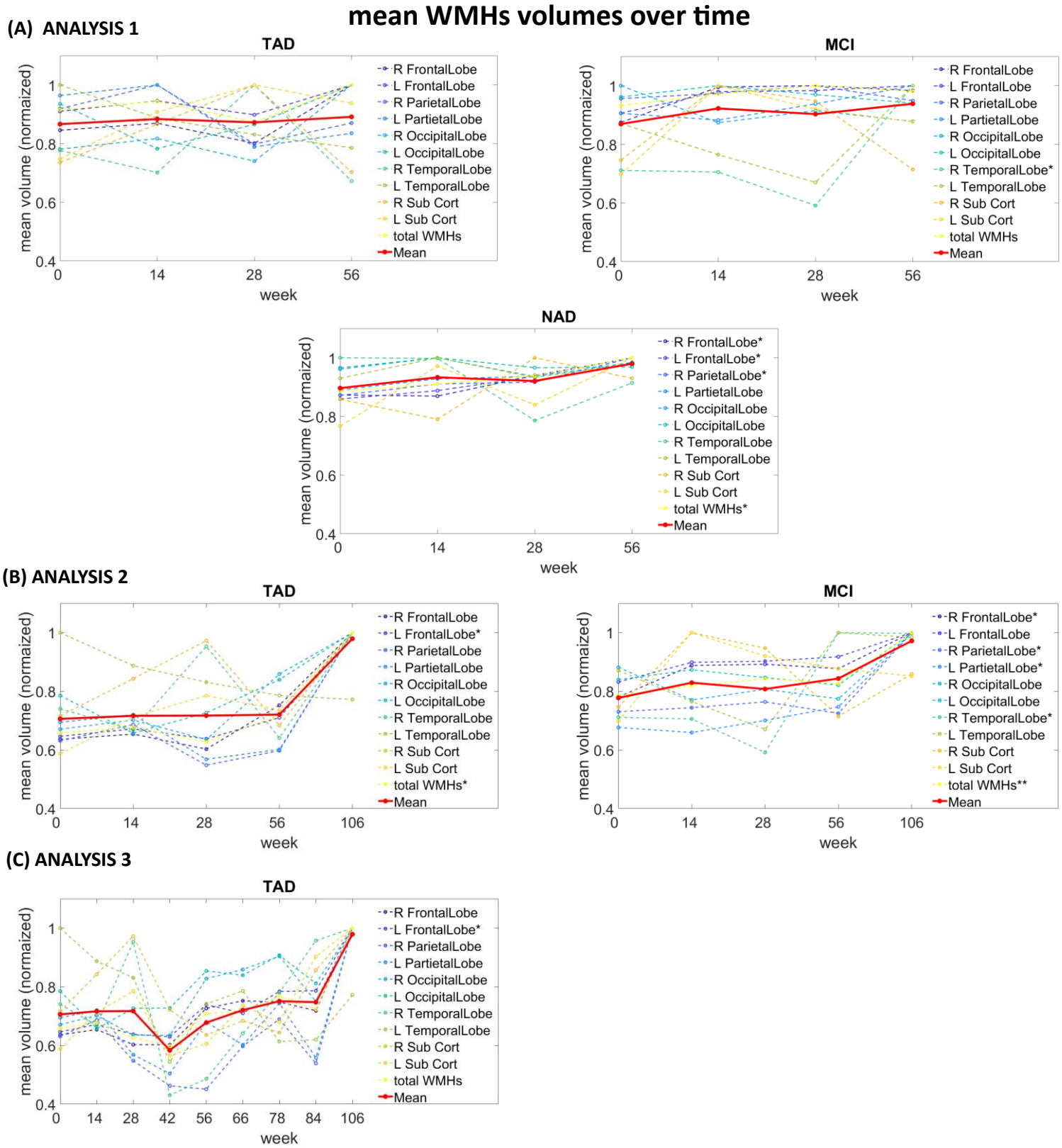


**Figure 4.** Mean lobar WMHs volumes in **A)** Analysis 1 (one year, four time points), **B)** Analysis 2 (two years, five time points) and **C)** Analysis 3 (two years, nine time points). * and ** Indicate significant ($p < .05$, $p < .001$) time effects. Generally, mean WMHs volumes in the TAD group do not increase significantly over time and progress with a pattern similar to MCI patients, suggesting a treatment effect especially during the first year of treatment (Analysis 1). The sudden decrease in mean volume for the TAD group in Analysis 3, week 42 is due missing data in one subject.

## DISCUSSION

*Regional Volumetry and Atrophy Rates*

We found hippocampal and parahippocampal baseline volumes in the TAD group to be greater compared with MCI subjects (Fig. 1A). This finding is consistent with studies reporting increased hippocampal atrophy in AD patients[9,26,27]. Baseline volumes of the same regions were not significantly different between the TAD and NAD groups, while other regions in the TAD group were often larger than in untreated subjects in the NAD group. Since the individuals in the TAD group previously underwent treatment with aducanumab, we suspect that the treatment could have decreased the degree of regional atrophy, resulting in smaller baseline volumes than untreated AD individuals.[51,52]

Conversely, as shown in Fig. 1A and 2A, the longitudinal analyses revealed that during the first year of treatment, the TAD group receiving aducanumab treatment exhibited severe regional atrophy, comparable to or even higher than the NAD group, in the majority of the ROIs (see Table 1 for a schematic view of the significant time changes and group differences of region volumes). Most of the ROIs in TAD patients showed significant atrophy over time, while only the hippocampus and anterior hippocampal gyrus exhibited significant atrophy in the NAD group. There were no statistically significant group differences between TAD and NAD patients, indicating that the atrophy patterns in treated and untreated AD patients were similar. Comparing TAD and MCI patients, we found a significant difference in hippocampal atrophy, consistent with previous studies highlighting the hippocampus as a key biomarker for AD[12,53]. The analysis over the two years of treatment revealed severe atrophy in the majority of ROIs in the TAD group, including the medial frontal cortex (Fig. 1B, 2B). Comparing TAD and MCI patients in the second year of treatment showed a greater degree of atrophy in the hippocampus, anterior parahippocampal gyrus, and prefrontal cortex regions of the TAD group. These results point out that the treatment does not slow down brain atrophy even after the clinical end point of 78 weeks. Lastly, the longitudinal analysis over all time points of the TAD dataset demonstrated significant atrophy in the same regions, although the progression of atrophy in the anterior cingulate cortex, precuneus, and angular gyrus appeared less severe compared to the previous analysis (Fig. 2C). We argue that the larger number of timepoints in this analysis made the volume loss appear more gradual, resulting in smaller p-values.

As expected from the regional volumetry results, we found the rates of annual atrophy in the TAD group to be comparable to the NAD group over the first year of treatment and significantly larger than in the MCI group over the two years of treatment. The hippocampal atrophy rates for the TAD and NAD groups were 1.5 to 2-fold larger than those reported in previous studies on AD patients[9]. We believe that the small sample size used in this study may have produced this discrepancy. Nevertheless, the atrophy rates of the parahippocampal gyri were consistent with previous findings (5-10% per year)[9]. These findings show that patients receiving aducanumab have atrophy patterns comparable to untreated AD subjects.

Overall, although the larger baseline volumes in the TAD group compared to the NAD group suggested that the antecedent aducanumab intake could have slowed down regional atrophy, our longitudinal results indicate that in the first year, the atrophy patterns in TAD patients closely resemble those of untreated NAD patients, suggesting no treatment effects. The significant group differences observed between TAD and MCI patients in the two years of treatment, along with the extensive atrophy in the TAD group, further emphasize that aducanumab does not mitigate the characteristic AD regional atrophy and the associated decay in cognitive abilities even after the clinical end point of the treatment.

*WMHs Volumetry*

Baseline WMHs volumes in the TAD group and MCI group were statistically similar except in the right frontal lobe, where they were smaller in the TAD subjects (Fig. 3A). These results are in contrast with previous findings reporting WMHs volumes to be larger in AD patients[51,52]. Further, the majority of the lobar WMHs volumes were significantly smaller in the TAD group than in the NAD group. Together, these results suggest that the earlier aducanumab intake of TAD patients could have limited the spreading of WMHs. However, these differences at baseline could be related to the different stages of AD and the age of the patients.

Similarly, our longitudinal analyses demonstrate that in the first year of treatment, TAD patients did not experience any significant increase in WMHs volumes (Fig. 3A, 4A, and see Table 2 for a schematic view of the significant WMHs time changes and group differences). Conversely, the NAD group showed severe growth in WMHs across all lobes and total WMHs, while MCI subjects experienced mild growth in WMHs in the right temporal lobe, which is overall consistent with earlier findings [5,14,19,29]. Although the group differences were not statistically significant, the absence of significant WMHs increases in the TAD group suggests a positive treatment effect. The analysis over the two years of treatment partially confirms these findings, as the TAD group showed significant yet less extensive and severe increases in WMHs volumes compared to the MCI group (Fig. 3B, 4B). The lack of significant group differences suggests that the time course of WMHs volume changes in treated patients is comparable to that observed in MCI subjects. Examining all time points of the TAD dataset reveals significant changes in WMHs only in the left frontal lobe, although Fig. 4C shows that all lobar WMHs are growing. Similarly to the regional analysis, we argue that the reduced number of significantly growing lobar WMHs in this analysis is likely due to the larger number of available time points, which smoothens the growth curve of WMHs.

In summary, our results from the WMHs volumetry indicate that in patients treated with aducanumab, the progression of WMHs is significantly less severe than in untreated AD patients and resembles the progression observed in MCI subjects. The lack of growth of WMHs in the parietal lobe suggests that aducanumab effectively removes NP, as previous studies reported WMHs volumes in this region to be highly correlated with NP burden[28]. These results may also explain the contained WMHs baseline volumes in the TAD individuals, as they already received aducanumab in the earlier ENGAGE and EMERGE trials.

Altogether, the findings from the regional volumetry and WMHs analyses provide valuable insights into the effects of aducanumab treatment on AD progression. The regional volumetry results demonstrate that aducanumab

does not prevent the neurodegenerative process (thus the subsequent cognitive decline) associated with AD during the first two years of treatment, as evidenced by the lack of impact on atrophy in critical brain regions like the hippocampus. On the other hand, the WMHs smaller baseline volumes and slower growth in treated subjects suggest that aducanumab may slow down the progression of AD-related damage to white matter tracts, potentially preserving structural and functional connectivity to some extent. We suggest that limiting the spreading and growth of WM damage could allow slowing down the decline in executive function, attention and psychomotor speed, verbal learning and memory, and semantic fluency typically associated with WMHs volumes in AD patients[19,21,28]. These findings contribute to our understanding of the limitations and potential benefits of aducanumab treatment in AD patients and may help explain the contrasting results from the ENGAGE and EMERGE trials conducted to test the efficiency of the aducanumab on global cognitive performance[1,35,36]. Finally, these results shed light on the role of NP in AD-related neurodegeneration by showing that NP burden may be the cause of WM damage, thus of the AD characteristic dysconnectivity[8,15–18].

There are several limitations to this study. First, the small sample size for all groups (n=13) may not allow to generalize the results. Further, the majority of the acquisitions in the NAD group only covered 56 weeks of disease, which is shorter than the clinical endpoint of 78 weeks that Biogen set[36,40]. This lack of time data potentially prevented us from uncovering additional effects of the treatment. Further, the fact that TAD subjects previously underwent aducanumab in earlier trials is a potential source of bias as it could have affected the time course of the disease. Finally, the lack of demographic data for the TAD group prevented us from exploring the effects of other relevant variables in AD studies, such as AD onset time, education level, ethnicity, E genotype, family history and diet[54,55].

Other AD structural and functional brain signatures could help measure the efficacy of the treatment in addition to the ones we treated in this work[7,8,11,53]. For instance, different studies reported that cortical thickness may predict AD-like cognitive decline and that WMHs are associated with subsequent cortical atrophy in regions that overlap with typical AD neurodegeneration patterns[11,20,53]. Moreover, resting-state fMRI studies have revealed altered connectivity networks in AD, particularly involving the default mode network (DMN)[7,13,17,18]. Finally, the connectivity of the language network was found to increase in early AD[15]. Due to time restrictions, the present study did not include the analysis of such additional AD features. Future studies should investigate the effects of aducanumab on NAD and TAD groups in terms of functional activity via functional MRI (fMRI) data, functional connectivity via diffusion MRI (dMRI) data, and cortical thickness to assess global effects of the treatment on the AD brain**.**

## CONCLUSION

We showed that aducanumab has no positive effects on the atrophy of commonly AD-affected brain regions in AD patients. However, the medication appears to significantly slow down WMHs growth, potentially mitigating the disruption of WM tracts during the first two years of treatment. These results indicate that NP removal is an effective yet partial solution to AD cognitive degeneration. Hence, as several studies suggest, the optimal treatment for AD most probably consists of a combination of NP removal and NFT removal[1,35]. Future works should investigate if the slower spread of WMHs in treated patients could help preserve the functional and structural connectivity than in untreated AD patients. In addition, patients receiving treatment should take cognitive tests that specifically measure skills that heavily rely on the integrity of white matter tracts in the parietal, occipital, and temporal regions of the brain to explore if the slower rate of WM damage leads to tangible cognitive advantages. These skills include working memory, attention and focus, processing speed, executive functioning, and visuospatial skills[28,56,57].

## ACKNOWLEDGEMENTS

I would like to thank Luis Marti-Bonmati for allowing me to carry out my project within his prestigious biomedical imaging group: GIBI2[30]. Furthermore, I warmly thank Leonor Cerda' Alberich for her supervision and Maria Beser for her highly valuable and professional daily supervision.

## REFERENCES

1. Vaz, M., Silva, V., Monteiro, C. & Silvestre, S. Role of Aducanumab in the Treatment of Alzheimer's Disease: Challenges and Opportunities. *Clinical Interventions in Aging* vol. 17 Preprint at https://doi.org/10.2147/CIA.S325026 (2022).
2. 2021 Alzheimer's disease facts and figures. *Alzheimer's and Dementia* **17**, (2021).
3. Iek Long, L., Wen, Z., Chin Ion, L., Chong, L. & Hong Lei, L. Macao Dementia Policy: Challenges and prospects (innovative practice). *Dementia* **20**, (2021).
4. Reid, A. T. & Evans, A. C. Structural networks in Alzheimer's disease. *European Neuropsychopharmacology* **23**, (2013).
5. Brickman, A. M., Muraskin, J. & Zimmerman, M. E. Structural neuroimaging in Alzheimer's disease: Do white matter hyperintensities matter? *Dialogues in Clinical Neuroscience* vol. 11 Preprint at https://doi.org/10.31887/dcns.2009.11.2/ambrickman (2009).
6. Lee, W. J. *et al.* Effects of Alzheimer's and Vascular Pathologies on Structural Connectivity in Early- and Late-Onset Alzheimer's Disease. *Front Neurosci* **15**, (2021).
7. Liu, Y. *et al.* Regional homogeneity, functional connectivity and imaging markers of Alzheimer's disease: A review of resting-state fMRI studies. *Neuropsychologia* **46**, (2008).
8. Matthews, P. M., Filippini, N. & Douaud, G. Brain structural and functional connectivity and the progression of neuropathology in Alzheimer's disease. *Journal of Alzheimer's Disease* vol. 33 Preprint at https://doi.org/10.3233/JAD-2012-129012 (2013).
9. Pini, L. *et al.* Brain atrophy in Alzheimer's Disease and aging. *Ageing Research Reviews* vol. 30 Preprint at https://doi.org/10.1016/j.arr.2016.01.002 (2016).
10. Amoroso, N. *et al.* Brain structural connectivity atrophy in Alzheimer's disease and for the Alzheimer's Disease Neuroimaging Initiative. *arXiv.org* (2017).
11. Dickerson, B. C. & Wolk, D. A. MRI cortical thickness biomarker predicts AD-like CSF and cognitive decline in normal adults. *Neurology* **78**, (2012).

12. Pennanen, C. *et al.* Hippocampus and entorhinal cortex in mild cognitive impairment and early AD. *Neurobiol Aging* **25**, (2004).
13. Shi, Y., Zeng, W., Deng, J., Nie, W. & Zhang, Y. The Identification of Alzheimer's Disease Using Functional Connectivity between Activity Voxels in Resting-State fMRI Data. *IEEE J Transl Eng Health Med* **8**, (2020).
14. Lee, S. *et al.* White matter hyperintensities are a core feature of Alzheimer's disease: Evidence from the dominantly inherited Alzheimer network. *Ann Neurol* **79**, (2016).
15. Pistono, A. *et al.* Language Network Connectivity Increases in Early Alzheimer's Disease. *Journal of Alzheimer's Disease* **82**, (2021).
16. Sun, Y. *et al.* Disrupted functional brain connectivity and its association to structural connectivity in amnestic mild cognitive impairment and alzheimer's disease. *PLoS One* **9**, (2014).
17. Dennis, E. L. & Thompson, P. M. Functional brain connectivity using fMRI in aging and Alzheimer's disease. *Neuropsychology Review* vol. 24 Preprint at https://doi.org/10.1007/s11065-014-9249-6 (2014).
18. Weiler, M. *et al.* Structural connectivity of the default mode network and cognition in Alzheimer's disease. *Psychiatry Res Neuroimaging* **223**, (2014).
19. Puzo, C. *et al.* Independent effects of white matter hyperintensities on cognitive, neuropsychiatric, and functional decline: A longitudinal investigation using the National Alzheimer's Coordinating Center Uniform Data Set. *Alzheimers Res Ther* **11**, (2019).
20. Karas, G. B. *et al.* Global and local gray matter loss in mild cognitive impairment and Alzheimer's disease. *Neuroimage* **23**, (2004).
21. Hirono, N., Kitagaki, H., Kazui, H., Hashimoto, M. & Mori, E. Impact of white matter changes on clinical manifestation of Alzheimer's disease: A quantitative study. *Stroke* **31**, (2000).
22. Bailly, M. *et al.* Precuneus and cingulate cortex atrophy and hypometabolism in patients with Alzheimer's disease and mild cognitive impairment: MRI and 18F-FDG PET quantitative analysis using FreeSurfer. *Biomed Res Int* **2015**, (2015).
23. Wu, X. *et al.* Altered default mode network connectivity in Alzheimer's disease-A resting functional MRI and Bayesian network study. *Hum Brain Mapp* **32**, (2011).
24. Zhou, B. *et al.* Impaired Functional Connectivity of the Thalamus in Alzheimer’ s Disease and Mild Cognitive Impairment: A Resting-State fMRI Study. *Curr Alzheimer Res* **10**, (2013).
25. Scahill, R. I. *et al.* A longitudinal study of brain volume changes in normal aging using serial registered magnetic resonance imaging. *Arch Neurol* **60**, (2003).
26. Apostolova, L. G. *et al.* 3D PIB and CSF biomarker associations with hippocampal atrophy in ADNI subjects. *Neurobiol Aging* **31**, (2010).
27. Waring, C. *et al.* Medial Temporal Atrophy on MRI in Normal Aging and Very Mild Alzheimer's Disease. *Neurology* **49**, (1997).
28. Brickman, A. M. *et al.* Regional white matter hyperintensity volume, not hippocampal atrophy, predicts incident Alzheimer disease in the community. *Arch Neurol* **69**, (2012).
29. Prins, N. D. & Scheltens, P. White matter hyperintensities, cognitive impairment and dementia: An update. *Nature Reviews Neurology* vol. 11 Preprint at https://doi.org/10.1038/nrneurol.2015.10 (2015).
30. Kuijf, H. J. *et al.* Standardized Assessment of Automatic Segmentation of White Matter Hyperintensities and Results of the WMH Segmentation Challenge. *IEEE Trans Med Imaging* **38**, (2019).
31. Dubois, B. *et al.* Advancing research diagnostic criteria for Alzheimer's disease: The IWG-2 criteria. *The Lancet Neurology* vol. 13 Preprint at https://doi.org/10.1016/S1474-4422(14)70090-0 (2014).
32. Park, G., Hong, J., Duffy, B. A., Lee, J. M. & Kim, H. White matter hyperintensities segmentation using the ensemble U-Net with multi-scale highlighting foregrounds. *Neuroimage* **237**, (2021).
33. Deture, M. A. & Dickson, D. W. The neuropathological diagnosis of Alzheimer's disease. *Molecular Neurodegeneration* vol. 14 Preprint at https://doi.org/10.1186/s13024-019-0333-5 (2019).
34. Selkoe, D. J. & Hardy, J. The amyloid hypothesis of Alzheimer's disease at 25 years. *EMBO Mol Med* **8**, (2016).
35. Walsh, S., Merrick, R., Milne, R. & Brayne, C. Aducanumab for Alzheimer's disease? *The BMJ* vol. 374 Preprint at https://doi.org/10.1136/bmj.n1682 (2021).
36. Nisticò, R. & Borg, J. J. Aducanumab for Alzheimer's disease: A regulatory perspective. *Pharmacol Res* **171**, (2021).
37. Mullard, A. Landmark Alzheimer's drug approval confounds research community. *Nature* **594**, (2021).
38. Jack, C. R. *et al.* The Alzheimer's Disease Neuroimaging Initiative (ADNI): MRI methods. *Journal of Magnetic Resonance Imaging* vol. 27 Preprint at https://doi.org/10.1002/jmri.21049 (2008).
39. Petersen, R. C. *et al.* Alzheimer's Disease Neuroimaging Initiative (ADNI): Clinical characterization. *Neurology* **74**, (2010).
40. Castrillo-Viguera, C. *et al.* EMBARK: A Phase 3b, Open-Label, Single-Arm, Safety Study to Evaluate the Long-Term Safety and Efficacy of Aducanumab in Eligible Participants With Alzheimer's Disease (2448). *Neurology* **96**, (2021).
41. Li, X., Morgan, P. S., Ashburner, J., Smith, J. & Rorden, C. The first step for neuroimaging data analysis: DICOM to NIfTI conversion. *J Neurosci Methods* **264**, (2016).
42. Manjón, J. V. *et al.* MRI denoising using Non-Local Means. *Med Image Anal* **12**, (2008).
43. Fernández Patón, M. *et al.* MR Denoising Increases Radiomic Biomarker Precision and Reproducibility in Oncologic Imaging. *J Digit Imaging* **34**, (2021).
44. Klein, S., Staring, M., Murphy, K., Viergever, M. A. & Pluim, J. P. W. Elastix: A toolbox for intensity-based medical image registration. *IEEE Trans Med Imaging* **29**, (2010).
45. Hutton, C., Draganski, B., Ashburner, J. & Weiskopf, N. A comparison between voxel-based cortical thickness and voxel-based morphometry in normal aging. *Neuroimage* **48**, (2009).
46. Salmond, C. H. *et al.* Distributional assumptions in voxel-based morphometry. *Neuroimage* **17**, (2002).
47. Good, C. D. *et al.* A voxel-based morphometric study of ageing in 465 normal adult human brains. *Neuroimage* **14**, (2001).
48. He, K., Zhang, X., Ren, S. & Sun, J. U-net: Convolutional networks for biomedical image segmentation," in International Conference on Medical image computing and computer-assisted intervention. *Lecture Notes in Computer Science (including subseries Lecture Notes in Artificial Intelligence and Lecture Notes in Bioinformatics)* (2015).

49. Knapp, H. ANOVA Repeated Measures. in *Practical Statistics for Nursing Using SPSS* (2023). doi:10.4135/9781506325651.n10.
50. Abdi, H. The greenhouse-geisser correction. *Encyclopedia of Research Design. Sage Publications* (2010).
51. Barber, R. *et al.* White matter lesions on magnetic resonance imaging in dementia with Lewy bodies, Alzheimer's disease, vascular dementia, and normal aging. *J Neurol Neurosurg Psychiatry* **67**, (1999).
52. Burton, E. J., McKeith, I. G., Burn, D. J., Firbank, M. J. & O'Brien, J. T. Progression of white matter hyperintensities in Alzheimer disease, dementia with Lewy bodies, and Parkinson disease dementia: A comparison with normal aging. *American Journal of Geriatric Psychiatry* **14**, (2006).
53. Fjell, A. M., McEvoy, L., Holland, D., Dale, A. M. & Walhovd, K. B. What is normal in normal aging? Effects of aging, amyloid and Alzheimer's disease on the cerebral cortex and the hippocampus. *Progress in Neurobiology* vol. 117 Preprint at https://doi.org/10.1016/j.pneurobio.2014.02.004 (2014).
54. Scarmeas, N., Luchsinger, J. A., Mayeux, R. & Stern, Y. Mediterranean diet and Alzheimer disease mortality. *Neurology* **69**, (2007).
55. Duara, R. *et al.* Alzheimer's disease: Interaction of apolipoprotein E genotype, family history of dementia, gender, education, ethnicity, and age of onset. *Neurology* **46**, (1996).
56. O'Dwyer, L. *et al.* Multiple indices of diffusion identifies white matter damage in mild cognitive impairment and Alzheimer's disease. *PLoS One* **6**, (2011).
57. M., P. *et al.* Assessment of white matter tract damage in mild cognitive impairment and Alzheimer's disease. *Human Brain Mapping* vol. 31 Preprint at (2010).